Cancer Letters 568 (2023) 216301

Contents lists available at ScienceDirect

Cancer Letters

journal homepage: www.elsevier.com/locate/canlet

R-spondin-3 promotes proliferation and invasion of breast cancer cells independently of Wnt signaling

Eline J. ter Steege [a], Loes W. Doornbos [a,1], Peter D. Haughton [a,1], Paul J. van Diest [a], John Hilkens [b], Patrick W.B. Derksen [a,**], Elvira R.M. Bakker [a,b,*]

[a] Department of Pathology, University Medical Center Utrecht, Utrecht, the Netherlands
[b] Department of Molecular Genetics, Netherlands Cancer Institute, Amsterdam, the Netherlands

ARTICLE INFO

Keywords:
R-Spondin-3
Breast cancer
Proliferation
Invasion
Wnt signaling

ABSTRACT

We recently identified R-spondin-3 (RSPO3) as a novel driver of breast cancer associating with reduced patient survival, expanding its clinical value as potential therapeutic target that had been recognized mostly for colorectal cancer so far. (Pre)clinical studies exploring RSPO3 targeting in colorectal cancer approach this indirectly with Wnt inhibitors, or directly with anti-RSPO3 antibodies. Here, we address the clinical relevance of RSPO3 in breast cancer and provide insight in the oncogenic activities of RSPO3. Utilizing the RSPO3 breast cancer mouse model, we show that RSPO3 drives the aberrant expansion of luminal progenitor cells expressing cancer stem cell marker CD61, inducing proliferative, poorly differentiated and invasive tumors. Complementary studies with tumor organoids and human breast cancer cell lines demonstrate that RSPO3 consistently promotes the proliferation and invasion of breast cancer cells. Importantly, RSPO3 exerts these oncogenic effects independently of Wnt signaling, rejecting the therapeutic value of Wnt inhibitors in RSPO3-driven breast cancer. Instead, direct RSPO3 targeting effectively inhibited RSPO3-driven growth of breast cancer cells. Conclusively, our data indicate that RSPO3 exerts unfavorable oncogenic effects in breast cancer, enhancing proliferation and malignancy in a Wnt-independent fashion, proposing RSPO3 itself as a valuable therapeutic target in breast cancer.

1. Introduction

The expression of the estrogen receptor (ER), progesterone receptor (PR) and human epidermal growth factor receptor 2 (HER2) are instrumental in breast cancer diagnosis and treatment, determining tumor subtype and intervention strategy respectively. Targeted therapies for breast cancer patients are largely directed against these receptors, of which the efficacy is challenged by tumor heterogeneity and therapy resistance. Moreover, triple negative breast cancers (TNBC) that lack expression of these three receptors are not susceptible for targeted treatments and hold relatively poor prognosis. To improve options for intervention strategies, it is crucial to obtain better insight into the molecular mechanisms that underlie breast cancer and to identify novel therapeutic targets.

In this perspective, R-spondin (RSPO) proteins, primarily known as agonists of the canonical Wnt/β-catenin pathway and regulators of stem cell niches, have emerged as clinically relevant oncogenes with apparent potential as therapeutic target [1]. Initially identified and recognized in the intestinal tract, pioneering (pre)clinical studies have mainly addressed the potential utility of targeting RSPO signaling in colorectal cancer [1–7]. These studies showed that both the direct targeting of RSPO ligands with monoclonal antibodies and the indirect targeting of Wnt signaling with porcupine inhibitors successfully reduced tumor growth and induced tumor differentiation in PDX models of colorectal cancer with a gain in *RSPO* [8–13]. Accordingly, in the mouse intestine, RSPO overexpression fueled tumor development, being accompanied by increased Wnt/β-catenin signaling and expansion of the proliferative stem cell compartment [14,15].

Interestingly, deregulation of RSPOs has also been linked to breast cancer, whereby overexpression of *RSPO2*, *RSPO3* and *RSPO4* have particularly been reported in patients with TNBC [9,16,17]. In agreement with these findings, we recently reported copy number

* Corresponding author. Department of Pathology, University Medical Center Utrecht, Universiteitsweg 100, 3584 CG, Utrecht, the Netherlands.
** Corresponding author. Department of Pathology, University Medical Center Utrecht, Universiteitsweg 100, 3584 CG, Utrecht, the Netherlands.
E-mail addresses: p.w.b.derksen@umcutrecht.nl (P.W.B. Derksen), e.r.m.bakker-8@umcutrecht.nl (E.R.M. Bakker).
[1] these authors contributed equally.

https://doi.org/10.1016/j.canlet.2023.216301
Received 5 June 2023; Received in revised form 27 June 2023; Accepted 2 July 2023
Available online 3 July 2023

amplifications of *RSPO2* and *RSPO3* in respectively 23% and 2% of breast cancer patients, which associated with lack of ER/PR expression, high tumor grade and reduced patient survival [18]. This association with receptor negative tumor status importantly indicates the potential clinical benefit that may be provided by RSPO as an alternative target in breast cancer. Additionally, we have recently reported that RSPO3 acts as a causal driver of breast cancer, as conditional overexpression of *Rspo3* in mouse mammary glands caused the consistent formation of poorly differentiated mammary tumors with metastatic potential [18]. We found that RSPO3-driven mammary tumors hold extensive differences in morphology and gene expression profiles compared to classical WNT1-driven mammary tumors, presenting as more malignant entities with relatively low Wnt activity [18]. In current study, we provide more insight in the activities through which RSPO3 drives breast cancer and the potential approach to target these activities, complementary using human breast cancer cell lines, an orthotopic transplantation model for human breast cancer, the RSPO3 breast cancer mouse model and tumor organoids models. We show that RSPO3 fuels increased proliferation and invasion of breast cancer cells, independent of Wnt signaling. Our data indicate that in breast cancer, RSPO3 functions as a Wnt independent and multi-faceted oncogene, presenting itself as a promising therapeutic target, whereas indirect targeting through Wnt inhibiton lacks therapeutic value in this setting.

2. Materials and methods

2.1. Transgenic and orthotopic transplantation mouse studies

Rspo3^{inv} mice (more detailed description of the *Rspo3*^{inv} mouse model provided in Ref. [14]) were crossed with MMTV-*Cre* mice [19], generating double transgenic MMTV-*Cre*;*Rspo3*^{inv} mice. The MMTV-*Wnt1* mouse model was kept in parallel [20]. Transgenic alleles were maintained heterozygous.

For the orthotopic transplantation study, B6;129*Rag2*$^{tm1F-wa}$*Il2rg*^{tm1Rsky}/DwlHsd immunodeficient mice (Envigo) were injected with 1x10^6 MCF7 pInducer hRSPO3 Flag/HA cells in the fourth mammary fat pad on the right side of each mouse. 24 h prior to fat pad transplantation, mice switched to β-estradiol containing water (4 μg/ml, Sigma). When tumors reached a volume of 50 mm^3, mice were randomized over two groups, either or not receiving doxycyline food (200 mg/kg, ssniff). Tumor volumes were monitored weekly and mice were sacrificed when tumors reached a volume of 1000 mm^3. All animal experiments were performed following Dutch legislation and with approval of the Animals Ethics Committee.

2.2. Immunohistochemistry

Isolated tissues were fixed in 4% formaldehyde for 24h and paraffin embedded. Hematoxylin eosin (HE) staining and immunohistochemistry (IHC) was performed according to routine protocols. For mouse tissues, the following antibodies were used: Ki67 (Abcam), p63 (D-9, Santa Cruz), Sox9 (Millipore), β-catenin (E247; Abcam), Cleaved Caspase3 (Asp175; Cell Signaling). IHC on transplanted human materials was performed on the Roche Ventana™ using K14 (SP53, Roche), K8 (B22.1, Roche), Ki67 (30-9, Roche), ERα (SP1, Roche) antibodies. Percentages of lung metastases were quantified by measuring the total surface area of all metastatic lesions and the total surface area of the lungs per mouse per section using Slide Score (Slide Score B.V.).

2.3. Flow cytometry

Isolated mouse tissues were kept in Hanks Balanced Salt solution (HBSS, Lonza) and minced using a Tissue Chopper (McIlwain). Tissue pieces were transferred to a digestion mix containing 3 mg/ml Collagenase type 3 (Worthington), 0.35 mg/ml Hyaluronidase (Sigma) and 0.1 mg/ml DNAse I (Stem cell technologies) in DMEM/F12 (Gibco) and left shaking at 37 °C for 1h. After digestion, red blood cells were removed using Red Blood Cell Lysis Buffer (BioVision). Cells were then incubated for 20′ at 37 °C in a solution of 1x Trypsin (Sigma) with 0.1 mg/ml DNAse I. Trypsin was inactivated by incubating the cells for 5′ at 37 °C in a solution of DMEM/F12, 10% FCS (Bodinco) and 0.1 mg/ml DNAse I. Single cells were then collected in HBSS using a 70 μm cell strainer (Falcon) and 500.000 cells were stained per condition. Cells were incubated with the primary antibodies for 30′ and with the secondary antibody streptavidin for 20' on ice in the dark. Antibodies used: CD49f-PerCP-Cy5.5 (GoH3, BioLegend), EpCAM (CD326)-BV510 (G8.8, BioLegend), CD61-PE-CY7 (2C9.G2 (HMβ3-1), BioLegend), TER-119-Biotin (TER-119, eBioscience), CD31 (PECAM-1)-Biotin (390, eBioscience), CD45-Biotin (30-F11, eBioscience) and Streptavidin-BV605 (BioLegend).

2.4. Generation of mouse tumor organoids

Isolated mammary tumors were collected in Advanced DMEM/F12 (Gibco) supplemented with 10 mM HEPES (Thermo Fischer), 1% Pen-Strep (Lonza) and 1% Ultra-Glutamine (Gibco) (AdDF+++). Tumors were minced into small pieces with a scalpel for approximately 50 times. Tumor pieces were placed in a Liberase digestion mix (0.1 mg/ml, Sigma) and left shaking at 37 °C for 1-1,5 h. Cells were spun down, washed with AdDF+++ and treated with 0.1 mg/ml DNAse I (Stem cell technologies) for 5′ at RT. Following, differential centrifuging was performed to select for epithelial tumor components. Finally, the epithelial organoids were placed in a 50 μl Basement Membrane Extract (BME, R&D Systems) hanging drop and left to polymerize for 45' at 37 °C before medium was added, being AdDF+++ supplemented with, 1x B27 (Thermo scientific), 1.25 mM N-Acetyl-L-cysteine (Sigma), 42.5 ng/ml FGF2 (Thermo Fischer) and 50 μg/ml Primocin (Invivogen).

2.5. Immunofluorescence

Cells and organoids grown in BME hanging drops were fixed with 4% PFA (Electron microscopy sciences) + 0.25% Glutaraldehyde (Sigma) to prevent degradation of the BME followed by treatment with 0.1% $NaBH_4$ to quench residual aldehyde groups after fixation. Organoids placed in a collagen-1 matrix were fixed with 4% PFA only. Samples were blocked in 0.3% Triton X-100 (Sigma) 5% normal goat serum (NGS, Sigma) in PBS (Sigma) for 1h at RT while rocking, followed by incubation with primary antibodies diluted in 0.3% Triton X-100, 1% BSA (Roche) in PBS for 24h at RT while rocking. Cells were washed 4 times 15' with PBS and incubated with secondary antibodies overnight at RT while rocking. Primary antibodies used: K14 (Poly19053, BioLegend), K8 (TROMA-I, Developmental Studies), GFP (D5.1, Cell Signaling), BrdU-Alexa Fluor® 647 (3D4, BD Biosciences). Secondary antibodies used: Anti-rat-Alexa-488 (Invitrogen), Anti-rabbit-Alexa-647 (Invitrogen). Immunofluorescence images were made using a Zeiss LSM880 microscope.

2.6. CellTiter-Glo assay

50,000 organoid-derived tumor cells were plated in a 50 μL BME hanging drop. Organoids were treated with DMSO control or 200 nM C59 (Cellagen Technology). At day 5, cell viability was measured using the CellTiter-Glo 3D cell viability assay (Promega) following manufacturers' protocol. Luminescence was measured using a spectrophotometer.

2.7. Invasion assay

RSPO3- and WNT1- driven tumor organoids were grown for 5 or 7 days in a BME hanging drop whilst treated with or without C59 (200 nM, Cellagen Technology). Next, cultures were incubated with 6 mg/ml Dispase (Gibco) for 20′ at 37 °C and reseeded in a Collagen-I matrix as

previously described [21]. After 24h, collagen gels were fixed for 10' with 4% PFA. Images were made using an EVOS M500 microscope using phase contrast.

2.8. Quantitative real-time PCR

RNA was extracted from organoids using Trizol (Life Technologies) and cDNA was synthesized using a transcription kit (BioRad iScript cDNA Synthesis Kit) according to the manufacturers' instructions. qPCR was performed using Fast Start Universal SYBR Green (Roche) on a BioRad CFX96 Real-Time system. The following primers were used: *Axin-2* F- 5′ GCTCCAGAAGATCACAAAG 3′, *Axin-2* R-5′ CTTCAGCATCCTCCTGTAT 3′, *Rspo3* F- 5′ AGATAGGAGTGTGTCTCTCTTCG 3′, *Rspo3* R- 5′ AGTATGATTGTTGGCTTCTAA CC 3'. *Actb* F- 5′ AGACCTCTATGCCAACACAG 3′, *Actb* R- 5′ CACAGAGTACTTGCGCTCAG 3'

2.9. Cell lines and medium

Cell lines were obtained from ATCC. MCF10A cells were grown in DMEM/F12 (Gibco) supplemented with 5% Horse serum (Fischer Scientific), 1% Pen/Strep, 20 ng/ml EGF (Peprotech), 100 ng/ml Cholera Toxin (Sigma), 10 μg/ml insulin (Sigma) and 0.5 mg/ml Hydrocortisone (Sigma). MCF7 and T47D cells were cultured in DMEM/F12 supplemented with 12% FCS, 1% Pen-Strep and 1% Ultra-glutamine.

2.10. Cloning and generation of stable cell lines

A pcDNA3.1 hRSPO3 Flag/HA vector (kind gift from the Clevers lab, Hubrecht institute, Utrecht, the Netherlands) was used as template to generate a hRSPO3 Flag/HA PCR product flanked by *BAMHI* and *ECORI* restriction sites. The resulting hRSPO3 Flag/HA PCR product was cloned into pEntry vector using GATEWAY cloning (Thermo Fisher Scientific). Subsequently, a LR reaction was performed, transferring the hRSPO3 Flag/HA sequence into the pInducer20 vector [22], generating pInducer hRSPO3 Flag/HA (pInd-hRSPO3). Wnt signaling reporter constructs used: 7TGP (7x Tcf-eGFP-Puro resistance cassette, #24305, Addgene) and 7TFP (7x Tcf-luciferase-Puro resistance cassette, #24308, Addgene). Stable cell lines were generated by lentiviral transduction followed by selection with appropriate antibiotic selection markers.

2.11. Immunoblotting

Cells were lysed in sample buffer, separated by SDS-PAGE and blotted. The following antibodies were used for immunoblotting: Flag (M2, Sigma) and GAPDH (Millipore). Detection was performed using IRDy680 goat anti-mouse antibody (Li-Cor) and the Amersham Typhoon Biomolecular Imager.

2.12. Growth and proliferation assays

MCF7 pInd-hRSPO3, T47D pInd-hRSPO3 and MCF10A pInd-hRSPO3 cells were treated with or without 1 mg/ml doxycyline 24h prior to the start of the experiment. 5,000 cells were plated in each 50 μl BME hanging drop. After BME polymerization, culture medium without or with doxycycline (1 mg/ml), Rosmantuzumab/OMP-131R10 (100 μg/ml, Proteogenix) or C59 (200 nM, Cellagen Technology) was added to the wells and medium was refreshed every other day. After 8 (MCF10A) and 10 (MCF7 and T47D) days, pictures were made of the 3D structures with an EVOS M500 microscope using phase contrast and cell surface area was measured using OrganoSeg [23].

For the BrdU incorporation assay, 10 μM BrdU (BD Biosciences) was added to the medium at day 5 (MCF10A) or day 8 (MCF7 and T47D). After 4h of incubation, cells were fixed 10′ with 4% PFA containing 0.25% glutaraldehyde. Fixed cells were treated with 2 M HCl for 90′ at RT followed by a 10' 0.1% $NaBH_4$ incubation step. Cells were then processed for immunofluorescence. The percentage of $BrdU^+$ cells was quantified using FIJI, counting the number of $BrdU^+$ and total number of nuclei (using DAPI) per 3D structure.

2.13. Luciferase assay

50,000 cells (MCF7 pInd-hRSPO3;TFP &T47D pInd-hRSPO3;TFP) or 20.000 cells (MCF10A pInd-hRSPO3;TFP) cells were plated per well in a 24-well plate. After 24h the culture medium was replaced by experimental medium containing either 1 mg/ml doxycycline (Sigma), 25% Wnt3a conditioned medium or a combination. 48h after stimulation luciferase activity was measured using the luciferase assay system (Promega) following manufacturers' protocol. A Berthold technologies Centro XS [3] LB 960 bioluminescencemeter was used for readout.

2.14. Statistics

Statistics were performed using two-sided Student's t-test in Graphpad Prism. Error bars indicate standard deviation (SD). Non-significant is indicated as ns, significance as $*p < 0.05$, $**p < 0.01$, $***p < 0.001$ and $****p < 0.0001$.

3. Results

3.1. RSPO3 fuels aberrant expansion of luminal progenitor cells during mammary tumorigenesis

To investigate the activities of RSPO3 in breast cancer, we used the conditional *Rspo3*^{inv} breast cancer mouse model that we recently published [14,18]. We previously characterized RSPO3-driven mammary tumors as poorly differentiated, and weak Keratin-5 (K5) and Keratin-8 (K8) staining patterns suggested that the solid tumor masses might largely consist of poorly differentiated luminal cells [18]. Staining for the luminal progenitor marker Sox9 demonstrated that the majority of the RSPO3-driven tumors is indeed Sox9-positive (Fig. 1A) [24], while basal cell marker p63 presented only in a minor subset of cells (Fig. S1A), together indicating the predominance of the luminal cell compartment in RSPO3 driven mammary carcinomas. Proliferation marker Ki67 revealed overt proliferative activity, especially in cells located along the edges of solid tumor masses (Fig. 1B). In contrast, apoptotic cells were rare, as indicated by low cleaved caspase-3 expression (Fig. S1B). β-catenin was expressed moderately in the RSPO3-driven tumors, being restricted to the cell membranes (Fig. 1C).

To further specify the cellular composition of RSPO3-driven breast carcinomas, we performed extensive flow cytometric analyses of RSPO3-driven tumors, neighboring mammary glands (MG) with RSPO3 overexpression and control mammary glands from mice lacking RSPO3 overexpression. Segregating $CD49f^{hi}EpCAM^{low}$ basal cells from $CD49f^{low}EpCAM^{hi}$ luminal cells, we observed an increase in the relative proportion of luminal cells in the mammary glands of MMTV-*Cre*;*Rspo3* mice compared to control glands (Fig. 1D and E). Moreover, RSPO3-driven mammary tumors displayed an even greater expansion of the luminal cell population, displaying an approximate 4-fold increased luminal-to-basal ratio (Fig. 1D and E). Following this confirmation of luminal expansion, we analyzed CD61, a marker for luminal progenitor cells that has been reported as cancer stem cell marker [24–28]. Segregating the luminal population into $CD61^-$ mature and $CD61^+$ progenitor luminal cells, we observed that in the non-neoplastic mammary gland, RSPO3 overexpression induced a significant increase in $CD61^+$ luminal progenitor cells (Ctrl MG: 0.6%, RSPO3 MG: 12.3%) which was further increased in RSPO3-driven mammary tumors (52.9%) (Fig. 1F and G). These data demonstrate that RSPO3-driven breast tumors are highly enriched in $CD61^+$ luminal progenitor cells, a feature that is unique to RSPO3 driven tumors, as this was not observed in WNT1-driven mammary tumors (Figs. S1C–D) [29]. Together, these data show that during mammary tumor development, RSPO3 drives the aberrant expansion of luminal progenitor cells marked by cancer stem

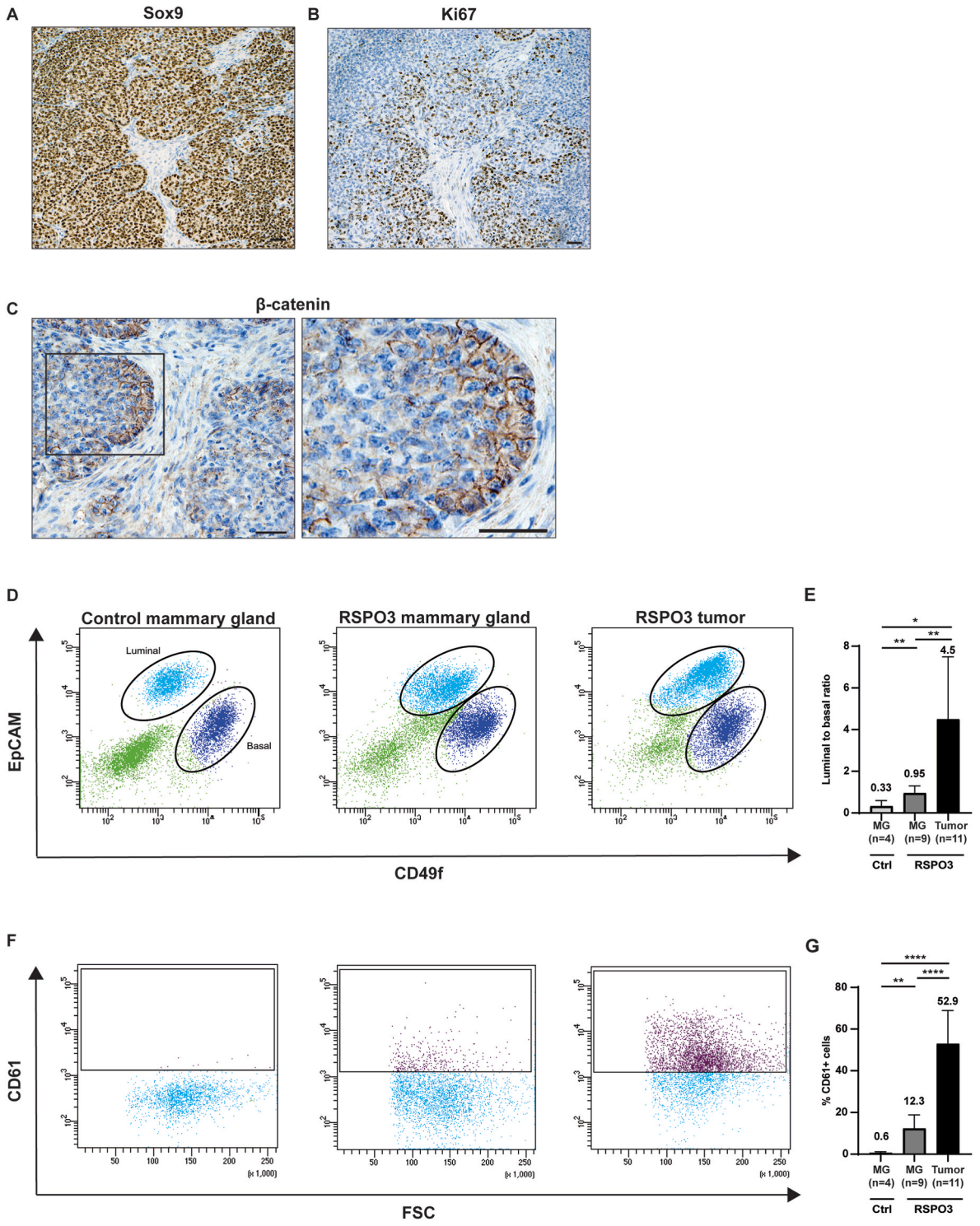

Fig. 1. RSPO3-driven mammary tumors are enriched in luminal progenitor cells
Immunohistochemical stainings for (A) Sox9, (B) Ki67 (20x objective) and (C) β-catenin (40x objective) on mammary tumors of MMTV-*Cre*;*Rspo3*^{inv} mice. (D–G) Flow cytometric analyses of mammary glands (MG) of single transgenic control (Ctrl) mice and mammary glands and tumors of MMTV-*Cre*;*Rspo3*^{inv} (RSPO3) mice. (D) FACS plots of mammary epithelial cells segregating luminal and basal populations and (E) average luminal to basal ratios. (F) FACS plots of the luminal cell population further specifying luminal progenitor cells based upon CD61 expression and (G) percentages of CD61^{+} cells.

cell marker CD61, distinctively from WNT1.

3.2. *RSPO3-tumor organoids grow independently of the Wnt signaling pathway*

To functionally investigate RSPO3 driven tumorigenesis *in vitro*, we generated mammary tumor organoids from MMTV-*Cre*;*Rspo3* and comparatively from MMTV-*Wnt1* mice (Fig. 2A). Increased *Rspo3* mRNA levels validated *Rspo3* overexpression in the RSPO3 tumor-derived organoids (Fig. S2A). Characterization of the RSPO3 tumor organoids with immunofluorescence revealed unevenly distributed expression of luminal marker K8 and basal marker K14 throughout the organoid

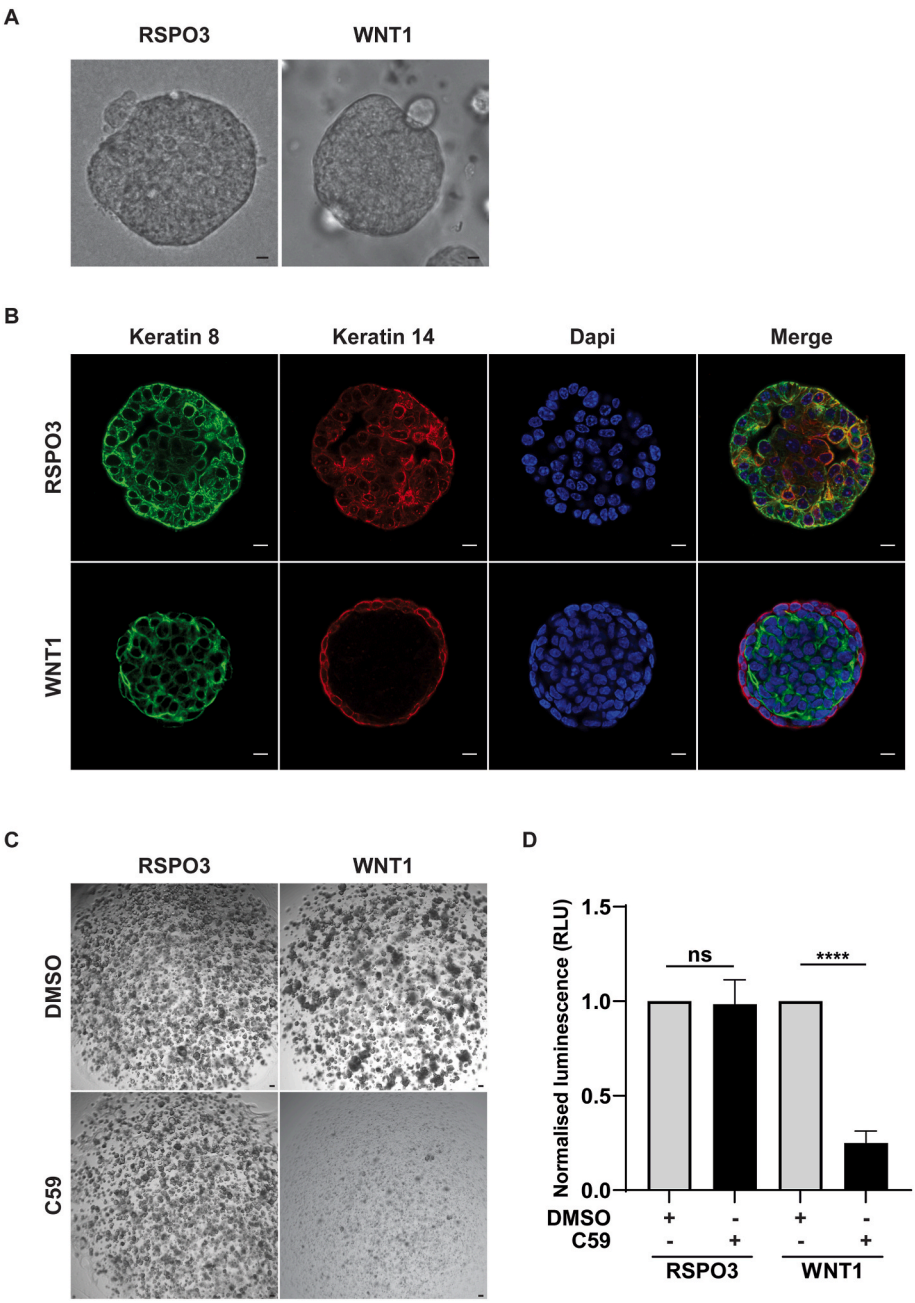

Fig. 2. RSPO3 tumor organoids are disorganized and grow independently of Wnt signaling (A) Representative brightfield images of RSPO3- and WNT1-driven mammary tumor organoids. Scale bars: 10 μm (B) Immunofluorescent staining of K8 and K14 on RSPO3 and WNT1- driven tumor organoids. Scale bars: 10 μm. (C) Brightfield images of RSPO3- and WNT1-driven tumor organoids treated with C59 for 5 days. Scale bars: 100 μm. (D) Normalized luminescence values of RSPO3- and WNT1- driven tumor organoids treated with C59.

structures, as well as hybrid cells expressing both keratins (Fig. 2B upper panel). This disorganized phenotype was unique to RSPO3 tumor organoids, as WNT1 tumor organoids displayed a distinct polarized keratin expression pattern indicating an outer layer of basal cells and an inner layer of luminal cells (Fig. 2B lower panel).

To investigate whether the growth of RSPO3-driven tumor organoids depends on Wnt pathway activity, we treated RSPO3- and WNT1 tumor organoids with porcupine inhibitor (PORCNi) C59 to inhibit both canonical and non-canonical Wnt signals. Interestingly, C59 had no effect on the growth of RSPO3 tumor organoids, indicating that RSPO3 driven mammary tumor cells proliferate independent of Wnt signals (Fig. 2C and D). Expectedly, the growth of WNT1 tumor organoids was drastically inhibited by C59 (Fig. 2C and D). Together these data demonstrate that RSPO3 mammary tumor-derived organoids recapitulate the disorganized *in vivo* tumor phenotype and grow independent of the Wnt signaling route.

3.3. RSPO3 potentiates proliferation of human breast cancer cells independently of Wnt signaling

To extrapolate above findings to human cells, we generated model systems of human breast and breast cancer, in which RSPO3 (tagged by Flag-HA) expression can be induced by doxycycline (Fig. 3A). We used the non-malignant breast epithelial cell line MCF10A, and the luminal breast cancer cell lines MCF7 and T47D, in which correct regulation of inducible RSPO3 overexpression upon doxycycline was confirmed by Western blot (Fig. 3B). Upon culturing these cell lines in 3D BME matrices, we consistently found that in all three models, RSPO3 overexpression induced a significant increase in growth (Fig. 3C and D). To synchronously visualize canonical Wnt pathway activation, we used a reporter construct containing 7 TCF sites with GFP [30]. In all three models we noticed that despite the growth stimulatory phenotype caused by RSPO3, RSPO3 expression did not induce TCF reporter expression by itself, but only when combined with Wnt3a ligand

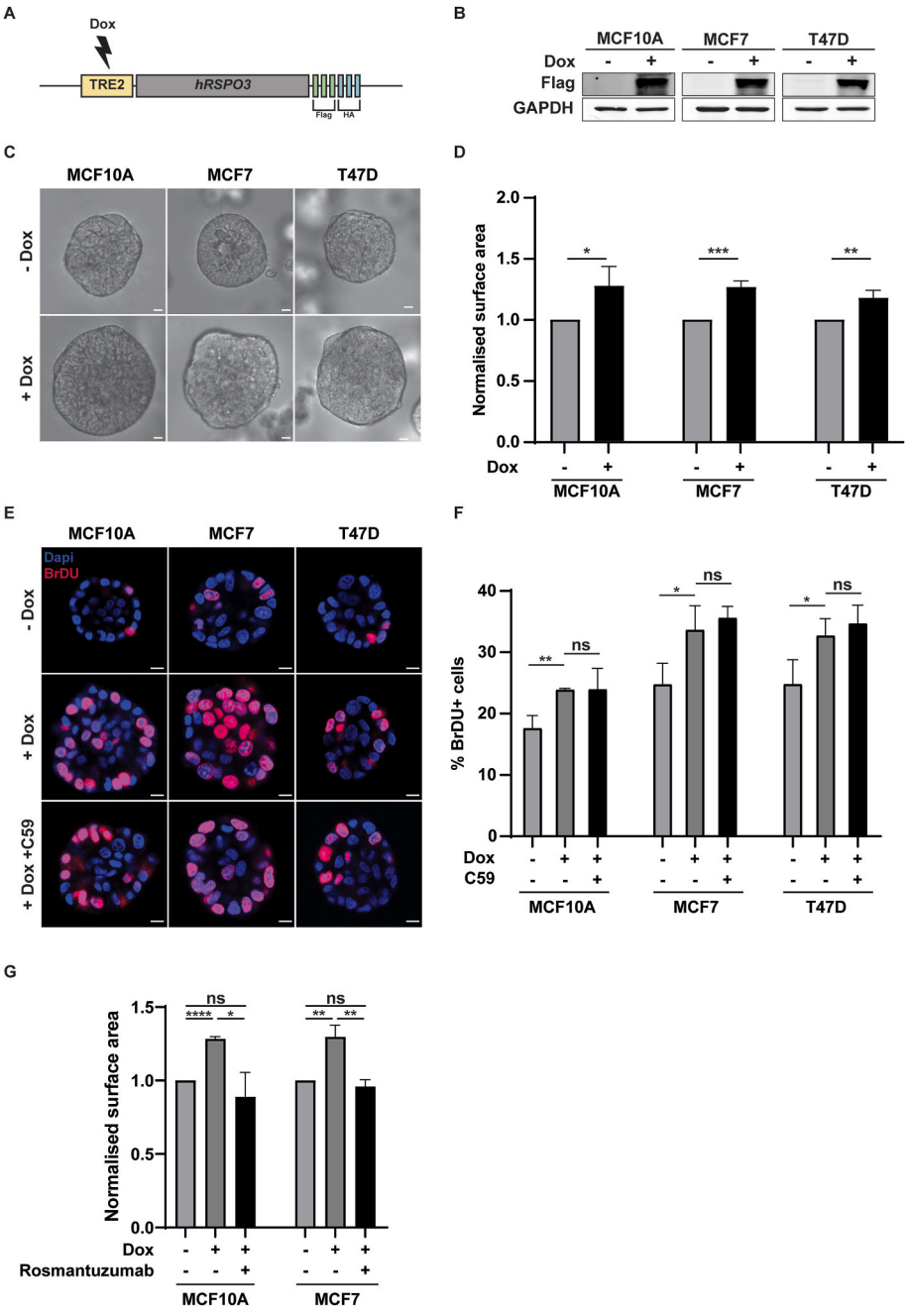

Fig. 3. RSPO3 drives proliferation of human breast cancer cell lines (A) Schematic representation of the inducible hRSPO3 Flag/HA construct introduced in breast cell lines. (B) Western blot for Flag confirming overexpression of RSPO3 upon treatment with doxycycline for 48h in MCF10A, MCF7 and T47D cell lines. (C) Representative brightfield images and (D) surface area quantifications of MCF10A, MCF7 and T47D cell lines upon RSPO3 overexpression at day 8 (MCF10A) and day 10 (MCF7, T47D). Scale bars, 10 μm. (E) Immunofluorescent staining and (F) quantifications of BrdU incorporation in MCF10A, MCF7 and T47D cells upon RSPO3 overexpression and treatment with PORCNi C59. Scale bars, 10 μm. (G) Surface area quantifications of MCF10A and MCF7 cell lines upon RSPO3 overexpression and Rosmantuzumab treatment at day 8 (MCF10A) and day 10 (MCF7). Scale bars, 10 μm.

stimulation (Fig S3 A-C). These findings show that RSPO3 promotes the growth of non-malignant breast and breast cancer cell lines independent of canonical Wnt signaling. An alternative Wnt/β-catenin reporter with luciferase as readout confirmed these results (Fig S3 D-F) [30].

To affirm the growth regulatory effect of RSPO3 to proliferation, BrdU incorporation was subsequently assessed. In accordance with the above results, all three cell lines show an increase in the percentage of $BrdU^{+}$ cells upon RSPO3 overexpression, demonstrating that RSPO3 promotes proliferation of human breast (cancer) cells (Fig. 3E and F). Moreover, C59-mediated inhibition of Wnt signaling did not affect the proliferation stimulatory effect of RSPO3 in all three cell lines (Fig. 3E and F), confirming that RSPO3 drives growth and proliferation of human breast cancer cells in a Wnt-independent fashion.

To test whether direct targeting of RSPO3 is a more effective strategy to inhibit growth, we executed the 3D growth experiment in the presence of the therapeutic anti-RSPO3 antibody Rosmantuzumab (OMP-131R10) that was previously tested in a clinical trial with colorectal cancer patients [31]. Importantly, treatment with Rosmantuzumab successfully inhibited the growth stimulatory effect of RSPO3 in both MCF10A and MCF7 cell lines (Fig. 3G), exemplifying the specificity of the obtained results.

3.4. *RSPO3-tumor organoids are highly invasive, independently of Wnt signaling*

As previously reported, RSPO3 overexpression induces mammary carcinomas that typically harbor EMT features and metastasize to the lungs [18]. To investigate the invasive potential *in vitro*, organoids derived from RSPO3-driven mammary tumors were placed in a Collagen-I dense matrix. RSPO3 tumor organoids were highly invasive, rapidly forming protrusions within 24 h (Fig. 4A). In contrast, WNT1 tumor organoids failed to invade in a collagen matrix, even after 5 days,

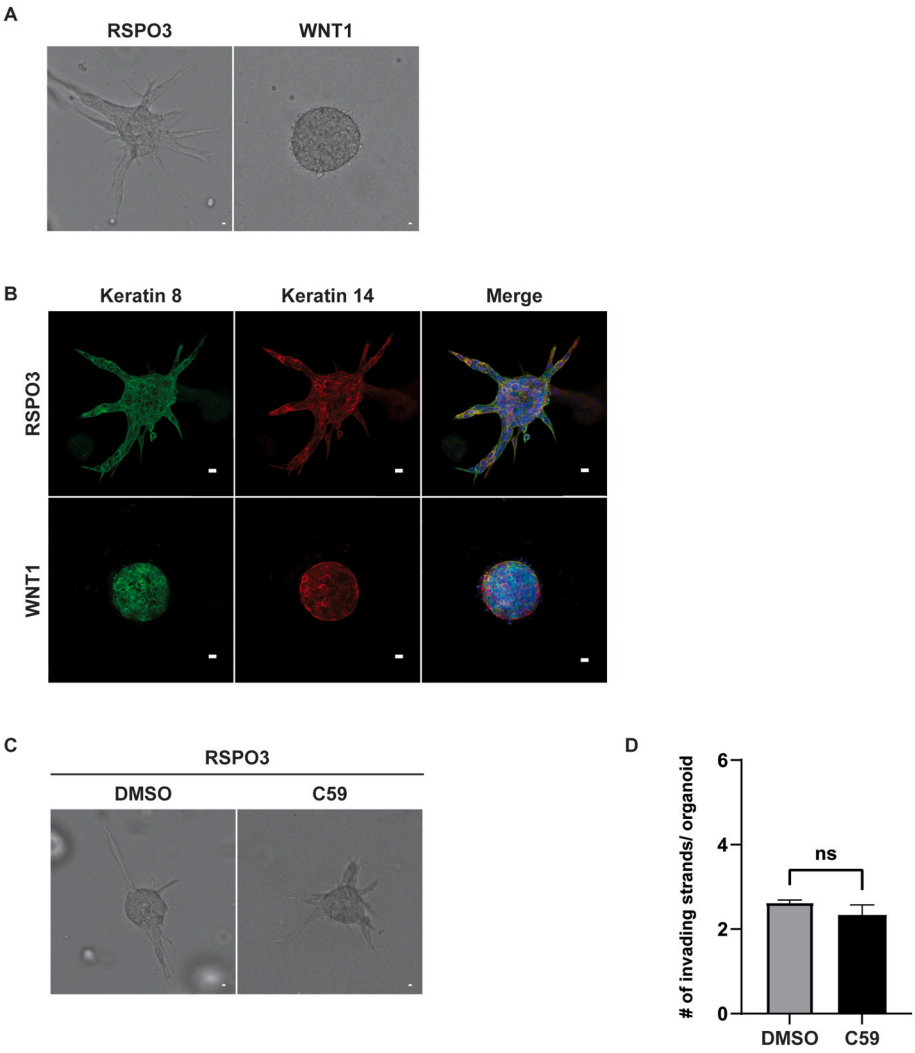

Fig. 4. RSPO3 drives invasion independently of Wnt signaling (A) Representative brightfield images of RSPO3- and WNT-1 driven tumor organoids grown in a collagen matrix for 24h. (B) Immunofluorescent staining for K8 and K14 on RSPO3- and WNT1- driven tumor organoids grown in a collagen matrix. Images are maximum intensity projections. (C) Brightfield images and (D) quantifications of the number of invading strands/organoid of RSPO3 driven tumor organoids in collagen upon C59 treatment. The number of invading strands were quantified 24h after collagen embedding in the presence of C59. Scale bars, 10 μm.

further confirming that the invasive phenotype is a feature specific for RSPO3 driven mammary tumors. Invasive RSPO3 tumor organoids retained a disorganized K8 and K14 expression pattern, with the invading strands of RSPO3 tumor organoids containing a mixture of $K8^+$, $K14^+$ and double positive cells (Fig. 4B). WNT1 tumor organoids maintained segregation of an outer layer of basal $K14^+$ cells and an inner layer of $K8^+$ luminal cells as in regular matrix (Fig. 4B).

To assess whether RSPO3-driven invasion depends on Wnt signaling, we performed the Collagen-I invasion assays in the presence of C59. Although C59 treatment effectively inhibited the Wnt pathway (Fig. S2B), the invading capability of RSPO3-driven tumor organoids was unaffected by C59 (Fig. 4C and D). This indicates that in addition to growth, RSPO3 also drives invasion independently of the Wnt signaling route.

3.5. *RSPO3 enhances distant metastasis of human breast cancer cells in vivo*

To investigate the effects of RSPO3 on human breast cancer cells in a preclinical *in vivo* model, we orthotopically injected MCF7 cells with the inducible RSPO3 overexpression construct in the mammary fat pads of mice. When xenografts reached a volume of 50 mm^3, mice were randomized into two groups receiving either normal or doxycycline food to induce RSPO3 overexpression. Tumor growth was followed over time until a volume of 1000 mm^3 was reached (Fig. 5A).

Induction of RSPO3 expression did not significantly affect the volume of primary mammary tumors (Fig. S4A). This is in contrast to our *in vitro* findings, which consistently indicated that RSPO3 enhances proliferation and growth of breast cancer cells. Most likely, this discrepancy resulted from the use of β-estradiol in the *in vivo* setting, commonly used to sustain tumor growth. β-estradiol also promotes tumor cell growth, masking the growth-stimulatory effect of RSPO3, as mimicked *in vitro* (Fig. S4B). Histological analysis of primary tumors developing in control and RSPO3 overexpression mice revealed high levels of K8, ER and Ki67 but no expression of K14, and no differences in expression levels of either staining between groups (Fig. S4C).

Interestingly, histological analysis of the lungs revealed enhanced distant metastasis in mice with RSPO3 overexpressing breast cancer cells, reaching an average of 7.8% of the lung area being covered by metastatic lesions, compared to 2.6% without RSPO3 overexpression (Fig. 5B and C). Corresponding to the primary tumors, metastatic lesions showed high levels of K8, ER and Ki67, no K14 and no differences in staining pattern between groups (Fig. S4D). These data demonstrate that RSPO3 overexpression is sufficient to enhance the metastatic potential of human breast cancer cells *in vivo* and suggest that RSPO3 targeting may be beneficial for intervention with RSPO3 driven breast cancer.

4. Discussion

Recently, we developed a mouse model for RSPO3-driven breast cancer, established RSPO3 as an oncogenic driver of breast cancer and demonstrated the consistent formation of poorly differentiated

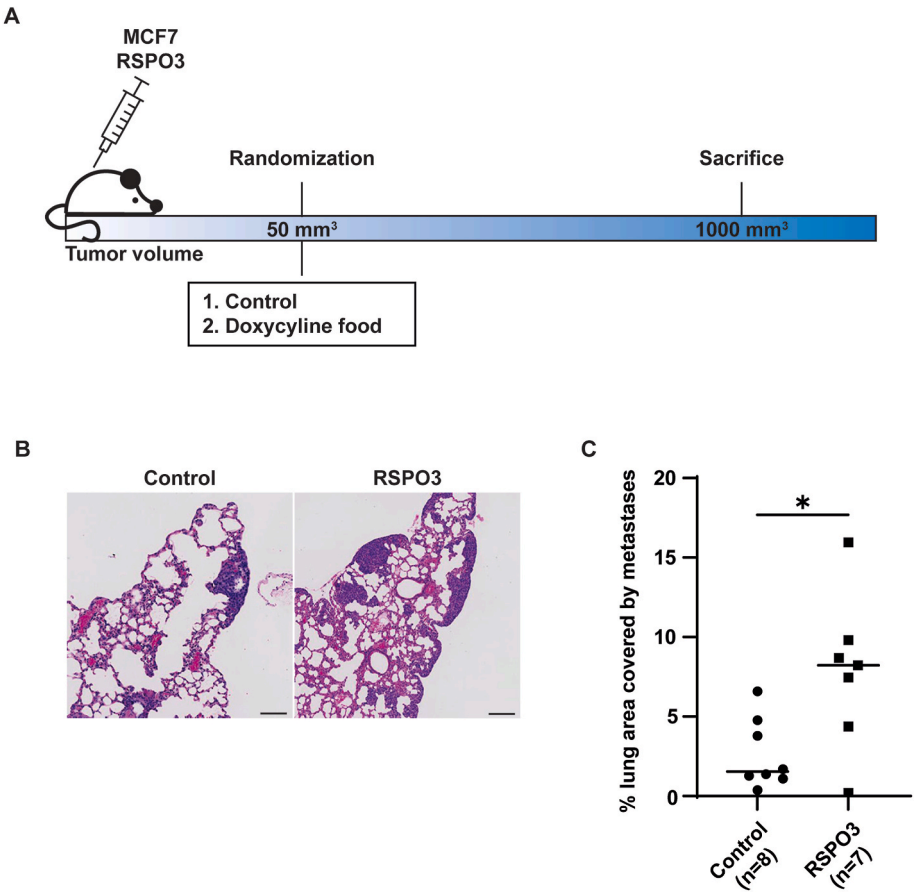

Fig. 5. RSPO3 enhances metastasis of human breast cancer cells *in vivo* (A) Schematic overview of the experimental set-up with control or RSPO3 overexpressing breast cancer cells (B) H&E stained sections of lungs with metastatic lesions. (C) Quantifications of the percentages of lung area being covered by metastatic lesions. Scale bars, 200 μm.

mammary tumors with high invading potential upon overexpression of *Rspo3* in the mouse mammary glands [18]. In human breast cancer, *RSPO* overexpression is particularly found in TNBC patients and accordingly we reported the presence of copy number alterations of *RSPO2* and *RSPO3* in respectively 23% and 2% of breast cancer patients that associated with ER and PR negative receptor status and high histological tumor grade [9,16–18]. Exploring the potential utility of RSPO3 as an alternative therapeutic target, we aimed to get more insight in the oncogenic activities through which RSPO3 contributes to breast cancer. Previously, we found that RSPO3-driven mammary tumors were poorly differentiated but had limited information on the cellular built-up [18]. Now, we show that RSPO3-driven mammary tumors are highly enriched in luminal progenitor cells marked by CD61. CD61 has been reported to mark luminal progenitor cells with highly enriched tumorigenic potential, as such being proposed as cancer stem cells [28]. Our data show that RSPO3 drives the aberrant expansion of luminal progenitor cells, potentially cancer stem cells. This stem/progenitor cell expanding activity exerted by RSPO3 in mammary tumorigenesis appears to align with the findings in the intestine, where RSPO3-driven cancer is associated with expansion of crypt stem- and progenitor cells [8,14,15]. This oncogenic activity appears as a deregulated extrapolation of RSPOs normal function in stem cell regulation [32,33]. Despite the seemingly comparable stem cell expanding activity of RSPO3 in the intestine and mammary gland, these organs differ greatly in their stem cell hierarchy, dynamics and regulation, with the mammary epithelium being instructed majorly by steroid hormones. In the mouse mammary gland, steroid hormones induce expression of RSPO1 in luminal progenitor cells, that in turn promotes mammary stem cell self-renewal in conjunction with WNT4 [32,34]. That implies that RSPO1 acts downstream of steroid hormone signals and as such might stimulate stem cell expansion independent of these upstream hormone signals in case of RSPO upregulation. In alignment, RSPO3 overexpression thus induced ER and PR negative mammary tumors highly enriched in $CD61^{+}$ luminal progenitor cells, or cancer stem cells.

In addition to the progenitor expanding effect exerted by RSPO3, our *in vitro* studies with tumor organoids and human breast cancer cell lines demonstrate that RSPO3 consistently promotes the proliferation, invasion and metastasis of breast cancer cells. With the identification of these oncogenic effects, we show that RSPO3 is involved in breast cancer development and progression, importantly adding up to previous reports that presented *Rspo3* as a tumor initiator in the mammary gland and to the clinical relevance as a potential therapeutic target [18,35–38]. As such, during continuation of our research we focused at the effects of RSPO3 on proliferation, invasion and metastasis, thus at tumor development and progression phases rather than initiation.

We investigated the role of Wnt signaling in RSPO3-driven breast cancer. Hence, potentiation of the Wnt/β-catenin pathway is the best known signaling activity of RSPOs, and in the intestine, this seems to occur during RSPO-driven tumorigenesis and can be successfully targeted using porcupine inhibitors [11–15]. However, in line with their different stem cell hierarchies, cancer developing in the intestine and breast represent very different diseases. Where colorectal cancer classically holds high levels of Wnt/β-catenin activation through *APC* or *CTNNB1* mutations, breast cancer is associated with a relatively lower degree of Wnt/β-catenin activation and underlying mutations are not often found [39–43]. Moreover, we previously reported lower expression of Wnt target genes in RSPO3-driven tumors compared to WNT1-driven tumors, indicating that RSPO3-driven tumors may be less

dependent on Wnt signaling activity [18]. Also, the morphology, invasive potential and gene expression profiles of RSPO3-driven mammary tumors differed greatly from that of WNT1 counterparts [18]. In this study, we demonstrate several effects exerted by RSPO3 during breast tumorigenesis and show that all of these were independent of Wnt signaling. No nuclear β-catenin translocation was observed in the RSPO3-driven mouse mammary tumors. With mouse organoid models, we showed that the growth of RSPO3 mammary tumor organoids is unaffected by treatment with PORCNi C59. Also, WNT1 derived organoids are non-invasive, whereas RSPO3 mammary tumor organoids were demonstrated to have high invasive capacity, which again could not be inhibited with C59. Then, with a novel panel of human breast cancer cell lines with inducible RSPO3 expression we showed that RSPO3 promotes growth and proliferation consistently *in vitro*. Utilizing reporters for canonical Wnt signaling, we showed that the growth stimulatory effect induced by RSPO3 did not coincide with reporter activity. Also, C59 was not able to inhibit the RSPO3-induced growth stimulatory effects. Together, these data consistently demonstrate that RSPO3 promotes proliferation and invasion of breast cancer cells in a Wnt-independent fashion. This further indicates that RSPO3 driven mammary tumorigenesis is not reliant on Wnt signaling, excluding both canonical and non-canonical as PORCNi C59 acts through inhibiting the functionality of all WNT ligands. This implies that in breast cancer with a gain in *RSPO*, indirect targeting with porcupine inhibitors will most likely be ineffective, in contrast to earlier findings in the intestine [11–13]. Instead, our data indicated that direct targeting of RSPO3 using the humanized monoclonal RSPO3 antibody Rosmantuzumab was effective in inhibiting the growth stimulatory effect of RSPO3 both in MCF10A and MCF7 cell lines, providing rationale to further investigate the potential of RSPO3 targeting in breast cancer.

In conclusion, we demonstrate that RSPO3 promotes growth and metastasis of breast cancer cells. As these unfavorable tumorigenic activities are exerted by RSPO3 in a Wnt independent manner, breast cancer patients with a gain in RSPO will not benefit from indirect targeting with Wnt inhibitors, but importantly, will expectedly benefit from treatment directly targeting RSPO3. This study provides solid rationale for (pre)clinical follow-up investigation to further assess the utility of RSPO3 as a therapeutic target in breast cancer.

CRediT authorship contribution statement

Eline J. ter Steege: Writing – original draft, Visualization, Validation, Software, Methodology, Investigation, Formal analysis, Data curation. **Loes W. Doornbos:** Visualization, Software, Methodology, Investigation, Formal analysis, Data curation. **Peter D. Haughton:** Software, Methodology, Investigation, Formal analysis, Data curation. **Paul J. van Diest:** Formal analysis, Resources. **John Hilkens:** Resources, Investigation, Formal analysis. **Patrick W.B. Derksen:** Resources, Methodology, Conceptualization, Formal analysis. **Elvira R.M. Bakker:** Writing – review & editing, Writing – original draft, Visualization, Validation, Supervision, Software, Data curation, Conceptualization, Formal analysis, Funding acquisition, Investigation, Methodology, Project administration, Resources.

Declaration of competing interest

The authors declare that they have no known competing financial interests or personal relationships that could have appeared to influence the work reported in this paper.

Acknowledgements

The authors thank the animal facilities of the Netherlands Cancer Institute (NKI) Amsterdam and the Gemeenschappelijk Dierenlaboratorium (GDL) in Utrecht. We are grateful for histology support from the NKI Animal Pathology Department and the UMC Utrecht Pathology Tissue Facility, for technical advice from the NKI Flow Cytometry Facility and technical assistance from Lotte Enserink. This work was financially supported by the Netherlands Organization for Scientific Research (NWO/ZonMW VENI 016.186.138) and the Dutch Cancer Society (KWF Young Investigator Grant 10957).

Appendix A. Supplementary data

Supplementary data to this article can be found online at https://doi.org/10.1016/j.canlet.2023.216301.

References

[1] E.J. ter Steege, E.R.M. Bakker, The role of R-spondin proteins in cancer biology, Oncogene 40 (2021) 6469–6478.
[2] S. Seshagiri, et al., Recurrent R-spondin fusions in colon cancer, Nature 488 (2012) 660–664.
[3] K. Shinmura, et al., RSPO fusion transcripts in colorectal cancer in Japanese population, Mol. Biol. Rep. 41 (2014) 5375–5384.
[4] T. Hashimoto, et al., EIF3E–RSPO2 and PIEZO1–RSPO2 fusions in colorectal traditional serrated adenoma, Histopathology 75 (2019) 266–273.
[5] Y. Mizuguchi, et al., Identification of a novel PRR15L-RSPO2 fusion transcript in a sigmoid colon cancer derived from superficially serrated adenoma, Virchows Arch. 475 (2019) 659–663.
[6] S. Sekine, et al., Comprehensive characterization of RSPO fusions in colorectal traditional serrated adenomas, Histopathology 71 (2017) 601–609.
[7] S. Sekine, et al., Frequent PTPRK-RSPO3 fusions and RNF43 mutations in colorectal traditional serrated adenoma, J. Pathol. 239 (2016) 133–138.
[8] E.E. Storm, et al., Targeting PTPRK-RSPO3 colon tumours promotes differentiation and loss of stem-cell function, Nature 529 (2016) 97–100.
[9] C. Chartier, et al., Therapeutic targeting of tumor-derived r-spondin attenuates b-catenin signaling and tumorigenesis in multiple cancer types, Cancer Res. 76 (2016) 713–723.
[10] M.M. Fischer, et al., RSPO3 antagonism inhibits growth and tumorigenicity in colorectal tumors harboring common Wnt pathway mutations, Sci. Rep. 7 (2017) 1–9.
[11] C. Li, et al., Identification of RSPO2 fusion mutations and target therapy using a porcupine inhibitor, Sci. Rep. 8 (2018) 1–9.
[12] B. Madan, et al., Wnt addiction of genetically defined cancers reversed by PORCN inhibition, Oncogene 35 (2016) 2197–2207.
[13] G. Picco, et al., Loss of AXIN1 drives acquired resistance to WNT pathway blockade in colorectal cancer cells carrying RSPO 3 fusions, EMBO Mol. Med. 9 (2017) 293–303.
[14] J. Hilkens, et al., RSPO3 expands intestinal stem cell and niche compartments and drives tumorigenesis, Gut 66 (2017) 1095–1105.
[15] T. Han, et al., R-Spondin chromosome rearrangements drive Wnt-dependent tumour initiation and maintenance in the intestine, Nat. Commun. 8 (2017) 1–12.
[16] F. Coussy, et al., Clinical value of R-spondins in triple-negative and metaplastic breast cancers, Br. J. Cancer 116 (2017) 1595–1603.
[17] J.M. Tocci, et al., R-Spondin3 is associated with basal-progenitor behavior in normal and tumor mammary cells, Cancer Res. 78 (2018) 4497–4511.
[18] E.J. ter Steege, et al., R-spondin-3 is an oncogenic driver of poorly differentiate invasive breast cancer, J. Pathol. 258 (2022) 289–299.
[19] K.U. Wagner, T. Ward, B. Davis, R. Wiseman, L. Hennighausen, Spatial and temporal expression of the Cre gene under the control of the MMTV-LTR in different lines of transgenic mice, Transgenic Res. 10 (2001) 545–553.
[20] A.S. Tsukamoto, R. Grosschedl, R.C. Guzman, T. Parslow, H.E. Varmus, Expression of the int-1 gene in transgenic mice is associated with mammary gland hyperplasia and adenocarcinomas in male and female mice, Cell 55 (1988) 619–625.
[21] T. Koorman, et al., Spatial collagen stiffening promotes collective breast cancer cell invasion by reinforcing extracellular matrix alignment, Oncogene 41 (2022) 2458–2469.
[22] K.L. Meerbrey, et al., The pINDUCER lentiviral toolkit for inducible RNA interference in vitro and in vivo, Proc. Natl. Acad. Sci. U.S.A. 108 (2011) 3665–3670.
[23] M.A. Borten, S.S. Bajikar, N. Sasaki, H. Clevers, K.A. Janes, Automated brightfield morphometry of 3D organoid populations by OrganoSeg, Sci. Rep. 8 (2018) 1–10.
[24] G.K. Malhotra, et al., The role of Sox9 in mouse mammary gland development and maintenance of mammary stem and luminal progenitor cells, BMC Dev. Biol. 14 (2014) 1–11.
[25] M.L. Asselin-Labat, et al., Gata-3 is an essential regulator of mammary-gland morphogenesis and luminal-cell differentiation, Nat. Cell Biol. 9 (2007) 201–209.
[26] G. Domenici, et al., A Sox2–Sox9 signalling axis maintains human breast luminal progenitor and breast cancer stem cells, Oncogene 38 (2019) 3151–3169.
[27] Wenjun Guo, Zuzana Keckesova, Joana Liu Donaher, Tsukasa Shibue, Verena Tischler, Ferenc Reinhardt, Shalev Itzkovitz, Aurelia Noske, Ursina Zürrer-Härdi, George Bell, Wai Leong Tam, Sendurai A. Mani, Alexander van Oudenaarden, R. W, Slug and Sox9 cooperatively determine the mammary, Stem Cell State 27 (2009) 417–428.
[28] F. Vaillant, et al., The mammary progenitor marker CD61/β3 integrin identifies cancer stem cells in mouse models of mammary tumorigenesis, Cancer Res. 68 (2008) 7711–7717.

[29] B. Teissedre, et al., MMTV-Wnt1 and -ΔN89β-catenin induce canonical signaling in distinct progenitors and differentially activate hedgehog signaling within mammary tumors, PLoS One 4 (2009).
[30] C. Fuerer, R. Nusse, Lentiviral vectors to probe and manipulate the Wnt signaling pathway, PLoS One 5 (2010).
[31] A Phase 1a/b Dose Escalation Study of the Safety, Pharmacokinetics, and Pharmacodynamics of OMP-131R10.
[32] C. Cai, et al., R-spondin1 is a novel hormone mediator for mammary stem cell self-renewal, Genes Dev. 28 (2014) 2205–2218.
[33] K.S. Yan, et al., Non-equivalence of Wnt and R-spondin ligands during Lgr5 + intestinal stem-cell self-renewal, Nature 545 (2017) 238–242.
[34] P.A. Joshi, et al., RANK signaling amplifies WNT-responsive mammary progenitors through R-SPONDIN1, Stem Cell Rep. 5 (2015) 31–44.
[35] V. Theodorou, et al., MMTV insertional mutagenesis identifies genes, gene families and pathways involved in mammary cancer, Nat. Genet. 39 (2007) 759–769.
[36] R. Callahan, et al., Genes affected by mouse mammary tumor virus (MMTV) proviral insertions in mouse mammary tumors are deregulated or mutated in primary human mammary tumors, Oncotarget 3 (2012) 1320–1334.
[37] C. Klijn, et al., Analysis of tumor heterogeneity and cancer gene networks using deep sequencing of MMTV-induced mouse mammary tumors, PLoS One 8 (2013) 1–10.
[38] A. Gattelli, M.N. Zimberlin, R.P. Meiss, L.H. Castilla, E.C. Kordon, Selection of early-occurring mutations dictates hormone-independent progression in mouse mammary tumor lines, J. Virol. 80 (2006) 11409–11415.
[39] C. Gaspar, et al., A targeted constitutive mutation in the Apc tumor suppressor gene underlies mammary but not intestinal tumorigenesis, PLoS Genet. 5 (2009).
[40] C. Gaspar, R. Fodde, APC dosage effects in tumorigenesis and stem cell differentiation, Int. J. Dev. Biol. 48 (2004) 377–386.
[41] E.R.M. Bakker, et al., β-Catenin signaling dosage dictates tissue-specific tumor predisposition in Apc-driven cancer, Oncogene 32 (2013) 4579–4585.
[42] E.H. van Schie, R. van Amerongen, Aberrant WNT/CTNNB1 signaling as a therapeutic target in human breast cancer: weighing the evidence, Front. Cell Dev. Biol. 8 (2020) 1–14.
[43] F.C. Geyer, et al., B-Catenin pathway activation in breast cancer is associated with triple-negative phenotype but not with CTNNB1 mutation, Mod. Pathol. 24 (2011) 209–231.